Firing Pattern and Spacing Burden Ratio Selection in Jointed Overburden Benches Using Unmanned Aerial Vehicle and Artificial Intelligence Based Tool

N. Sri Chandrahas[1(✉)], B. S. Choudhary[2], and M. S. Venkataramayya[1]

[1] Mining Engineering Department, Malla Reddy Engineering College, Hyderabad, India
srichandru2009@gmail.com

[2] Mining Engineering Department, IIT(ISM) Dhanbad, Dhanbad, India

Abstract. The distinct effects of rock joints and the initiating firing pattern on the consequences of blasting in terms of rock fragmentation and generated ground vibration are both substantial. The integrated consideration effect of rock joints along with the spacing burden ratio and firing patterns, which enables access to the most beneficial and secures blasting outcomes, has not received much research. To adopt the optimal firing pattern to lower mean fragmentation size (MFS) and peak particle velocity (PPV), rock joints were therefore examined and evaluated in this research using scientific methods. In order to carry out the research stated goal, 90 blast experiments were carried out at the various mines. When joints are perpendicular to the free face, the results showed that MFS and PPV are greatly reduced when shot perpendicularly (V firing pattern) with lesser spacing burden ratio. When joints are also parallel to the free face while firing in a similar pattern, good results are seen with higher spacing burden ratio.

Keywords: UAV · Joints · Firing Patterns · MFS and PPV

1 Introduction

Rock qualities, explosive properties, the initiation mechanism, blast geometry factors, and so on are all examples of the various parameters that might affect the fragmentation and other effects like ground vibration. To maximize the outcomes of blasting in terms of the lowest environmental consequences like ground vibration and acceptable size of rock fragmentation, the focus should be placed on controllable (Blast design parameters) and uncontrollable parameters (Rock mass characteristics). So when planning the blasting pattern, it is essential to take into account a variety of elements, including the front-row burden, the burden, the spacing, the depth of a hole, the stemming column, the decking length, and the firing pattern [1–6]. Rock mass properties like joint plane spacing and the orientation of the joint planes are the factors those influence rock fragmentation and ground vibration [7, 8].

B. Raj et al. (Eds.): ICETE 2023, AER 223, pp. 1334–1358, 2023.
https://doi.org/10.2991/978-94-6463-252-1_134

At the moment an explosive charge is set off, its components are instantly turned into gases with extreme temperature and huge pressure. When high-pressure gases hit the wall of the blast hole all at once, the shock wave is sent through the rock mass. Fractures form in the rocks around the outgoing shock wave if the stress is stronger than the rock's dynamic compressive strength [9]. It also gets radial cracks because of bending and pulling forces [10]. When a compressive stress wave hits an open joint or a free face, when the tensile wave bounces off of a rock's dynamic strength, it becomes stronger [11, 12]. Reflections of the compressive wave make tensile and shear waves, which can move through cracks and make them bigger [13] as shown in Fig. 1 (a, b, c & d). This is because the discussed two types of waves have different phases. After a stress wave spreads, high-temperature, high-pressure gases expand the original borehole, make radial cracks longer and let them go deeper, or go through natural cracks in both. The high-pressure gases break open and widen these cracks. Explosive gases entangled in the rock mass nudge the rock mass forward and potentially trigger flexural rupture by bending the face [14]. The discussed concept of rock breakage may not as same as in disturbed rocks like joints [8, 15, 16]. Damage to rock masses is likely to result from these weak planes such as joints and bedding planes [17].

Making ensuring that chosen blast design parameters adhere to all post-blast environmental restrictions and the targeted fragmentation needed for mine and mill is a difficult issue for blasting engineers. Together with fragmentation, ground vibration is a significant problem that has to be addressed. By balancing explosive energy to rock strength, appropriate blast hole size and geospatial location, and other blast design factors, great increases in blast performance can be achieved. Unfortunately, Geo–blast parameters includes burden spacing ratio, firing pattern and joint angle have an enigmatic effect on both fragmentation and ground vibration. It indicates that a minor change in one parameter causes divergent effects in rock fragmentation and generated ground vibration at the same time; for instance, when fragmentation improves, the small adjustment dramatically increases peak particle velocity [18].

The most prevalent and most crucial from geotechnical perspective discontinuities in rocks are joints. Joints are fractures of natural deposits across whereby there has little or no evident relative displacement [19, 20]. The greater number of joints in a rock mass has an effect not only on the rock's mechanical qualities but also on its dynamic responsiveness [21] shown in Fig. 2. When a stress wave comes into contact with a rock mass that has any kind of discontinuity, it instantly loses energy and begins to attenuate. For this reason, it is of the utmost significance to do a study into the connection between the number of rock joints and their quality [22]. The existence of jointing in a rock formation has a significant influence both on the rock's MFS and the blast's overall safety [23]. Similarly, rock joints have a prominent influence on the transmission of shockwaves following blasting [1].

The incidence angle about the joint face influences the rate of attenuation of stress waves in joints [24, 25]. Attenuation of stress waves will be caused in a different direction depending on the angle from which the rock joint is seen. In most cases, normal angle 90° is responsible for the very rapid attenuation of stress waves [26]. As the incidence angle increases, the transference coefficient consistently decreases, but the backscatter coefficient steadily increases up to the incident angle and continues to climb as it

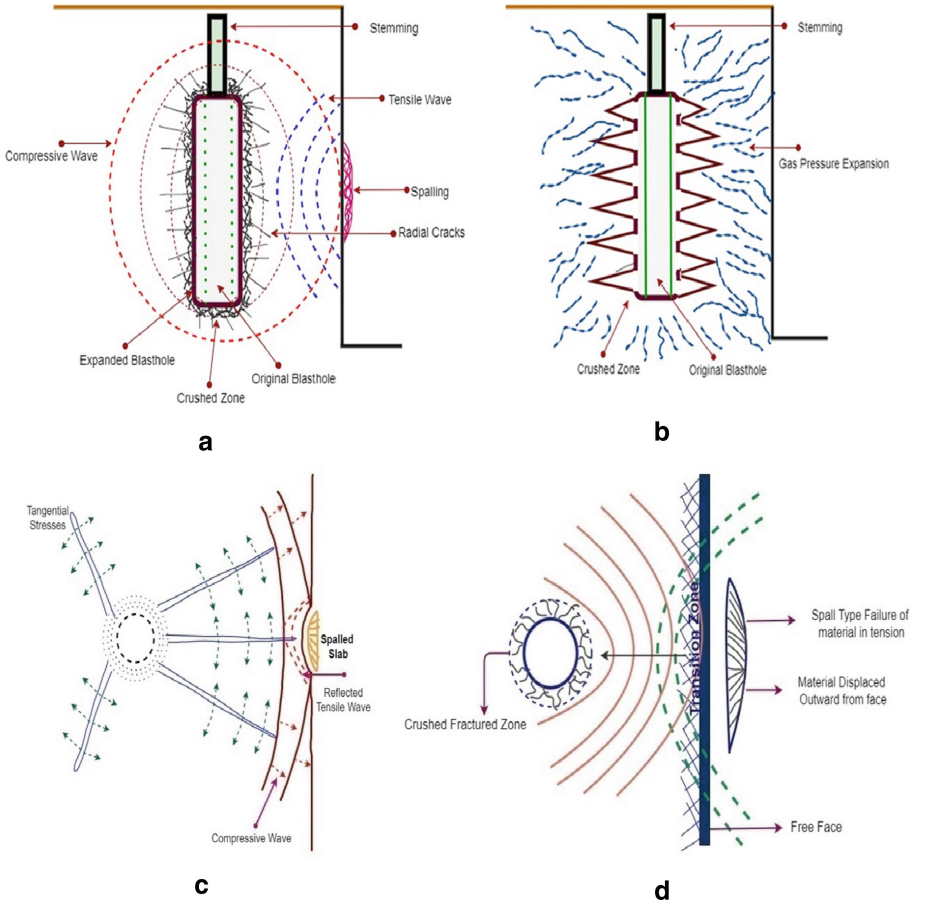

Fig. 1 (a) Shock wave propagation (b) Gas pressure expansion (c) Reflection of tensile waves and spalling & (d) Final fractured zone

moves closer and closer to the critical angle of 90° [27]. The wave transference and backscattering both affected the incidence angle as a result. In such conditions firing perpendicular to joint facilitate proper explosive consumption and better casting [7], as shown in Figs. 5 and 6. In addition to affecting fragmentation; the joint angle can also affect ground vibration. A change in joint angle has a substantial enough impact on the blast vibration to be regarded as important since it may result in a change in the attenuation rate of vibration velocity (Rinehart et al., 1958). The touching angle, waveform pattern, and structural characteristics of the rock joint will determine how a blast stress wave interacts with it, and these elements may cause the blast energy to be dispersed [26, 28].

It is obvious that the mean fragment size of the blasted rock decrease as the spacing to burden ratio rises. This might be as a result of the explosive's firing, which results in an increase in spacing and a decrease in burden value [29]. The thin ledges of rock mass that

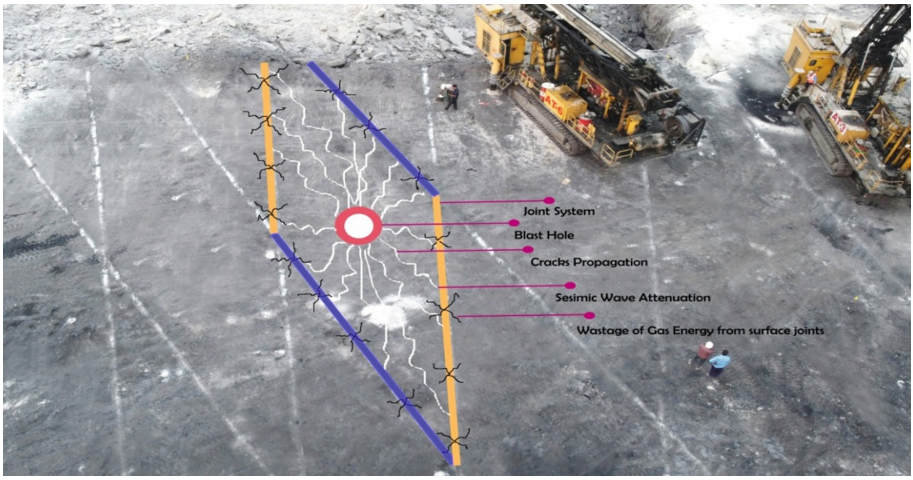

Fig. 2 Understanding the effect of joints on rock breakage at opencast coal mines at ramagundam III, SCCL.

resulted in the reduced fragmentation were produced by increased spacing and decreased burden. The spacing to burden ratio typically ranges from 1 to 2, but the ideal values were 1.15 for staggered patterns and 1.25 for rectangular patterns [30]. The optimum value of spacing to burden ratio in most of the blasts ranges 1.1 to 1.3 and it results into good fragmentation [31]. In accordance, the spacing burden ratio had a significant influence on induced ground vibration [32]. Excessive spacing burden might trigger scope to propagate unnecessary peak particle velocity [33]. Detonation waves need a route to follow to get to the explosives stored in the holes; this is what a firing pattern does. The most important aspect of any blasting program is the successive formation of the free face. As a result, the firing pattern determines rock movement and direction by allowing the following blast holes/rows to be positioned on a free face [30, 34]. Other aspects like ground vibration, the proper application of the pattern can help achieve the best results possible. A concept to consider firing burden and spacing-to-burden ratio for deciding firing pattern produces significant results [35].

Important factors affecting the mean fragmentation size include, in addition to joint spacing, the influence of joint angle [36]. Poor rock fragmentation occurred when the wave front path at an angle to the joint plane. On the other hand, when the blast was pointed in a path that was parallel to the plane of weakness, excellent rock fragmentation was created. In many situations, better fragmentation was found to occur when the free face was oriented so that it was parallel to the joint planes shown in figure 2.22 [37]. In addition to affecting fragmentation, the joint angle can also affect ground vibration. A change in joint angle has a substantial enough impact on the blast vibration to be regarded as important since it may result in a change in the attenuation rate of vibration velocity. The touching angle, waveform pattern, and structural characteristics of the rock joint will determine how a blast stress wave interacts with it, and these elements may cause the blast energy to be dispersed [38].

Attenuation of stress waves will be caused in a different direction depending on the angle from which the rock joint is seen. In most cases, normal angle 90^0 is responsible for the very rapid attenuation of stress waves [26]. As the incidence angle increases, the transference coefficient consistently decreases, but the backscatter coefficient steadily increases up to the incident angle and continues to climb as it moves closer and closer to the critical angle of 90^0 [27]. The wave transference and backscattering both affected the incidence angle as a result. In such conditions firing perpendicular to joint facilitate proper explosive consumption and better casting, shown in Fig. 6.

Data collecting using UAV technologies has produced more accurate outcomes in numerous scientific domains [39]. UAV technology has recently been adopted into the mining industry to perform volume calculations, terrain monitoring, and surveying. Geological formations were quantified and described using photogrammetric data [40]. A study demonstrated the use of photogrammetric methods to map the locations of geological joints. Using UAV technology, it is possible to gather topographic data with millimeter- to centimeter-level resolution over areas measuring many square kilometers [41]. UAV technology is inexpensive and user-friendly. In structural analysis, a 3D point cloud is used to extract 3D structural data in order to understand the strike and dip of fractures [42, 43]. Employed UAV datasets and cutting-edge software to locate joints, faults, and fractures in dip and strike orientations. A novel least-cost-path method was also developed by [44] to map geological structures like joints using UAV information. Moreover, fragmentation can be mapped more precisely than with conventional techniques [40]. Analogously, computational technologies also play an effective role in the measurement and prediction of joints nowadays [45]. Face mapping technology combination of drone photography and AI software assessment can result in optimal fragmentation with permitted PPV [46]. Unmanned Aerial Vehicles (UAVs) or drones are useful in locating joint planes and other geological discontinuities that may aid in blast design [38].

2 Materials and Methods

2.1 Field Data Collection

Experiments were carried out at the opencast mine II, Ramagundam, owned by Singareni Collieries Company Limited and the kesoram limestone mines. The mine is located at latitudes 180 39’ 07" N and 180 41’ 05" N, and longitudes 790 32’ 37" E and 790 33’ 53" E. The mining zone is surrounded by a rather thick layer of soil, alluvium, and sandy soil, as well as various different types of rocks that are part of the Barakar Formation and belong to the Lower Gondwana group. Blast hole section and firing pattern used in the experimentations were shown in Fig. 3 (a & b).

2.2 Data Analysis

Artificial intelligence (AI) software recognized joint planes, dip angles, and intervals to examine the target bench’s joint intensity and joint pattern as shown in Fig. 4 (a, b & c). The primary algorithm of the software was designed primarily to look through the collected data for specific qualities associated with rock joints.

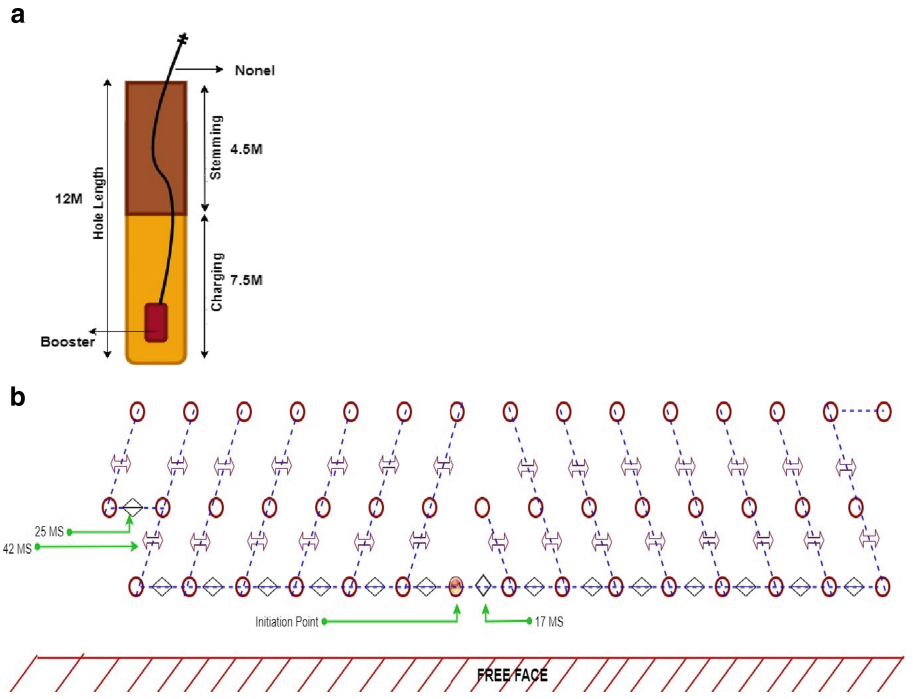

Fig. 3. (a) Blast Hole Section (b) Staggered Drilling with V Firing Pattern at Mine A

The model bench depicted in Fig. 4 was photographed at one of the experimental sites at the KESORAM limestone mine in Basantnagar, Telangana. The model was built with the help of approximately 25 images taken at the area where the data was obtained.

2.3 Blast Experimentation

To accomplish the primary goal of this study, blasts have been carried out using the blasts that were developed in AI-based software. There were a total of 90 blasts carried out on 05 benches consisting of sedimentary rocks such as coal (Overburden) and limestone; several different combinations of blasts were carried out so that the individual trends and their effects on rock fragmentation and ground vibration could be seen simultaneously.

Phase I: All blast design parameters are maintained the same, but the firing pattern is altered with the respect to joint angle.

Phase II: All blast design parameters are maintained the same, but the Spacing Burden Ratio is altered with the respect to joint angle.

Phase V: All blast design parameters are maintained the same, but the firing pattern and spacing burden ratio together are altered concerning the joint angle.

In the beginning, each of the experiment benches was cleaned to a depth of 0.3 meters to improve the joint visibility on the bench for identification and reference

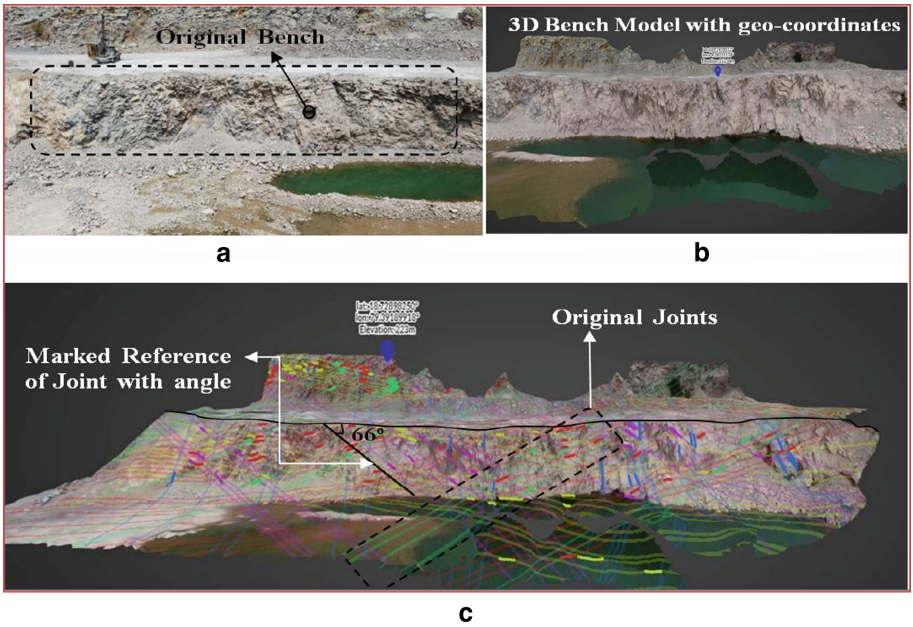

Fig. 4 (a) Original bench image captured by drone used for model creation (b) 3D model created in AI software (c) Joint detected in software of the limestone bench at Kesoram Limestone Mines, Basant Nagar, Telanagana

marking. This method is particularly useful in mines that have been worked underground in the past when there is a greater potential for the formation of fractures and the disruption of the strata. An L&T 9020 Dozer was used to clear the area and level the ground. The same procedure was carried out at each of the mine's experiment benches. To maintain accuracy throughout the experiment, the marking of joints on the bench was performed on every respective bench, and proper scales and measurement kinds were used. To avoid perturbation caused by wind turbulence and other climatic issues, two-step marking with white powder was used.

After the joint planes had been effectively identified, the burden and spacing had to be accurately estimated to avoid overlapping drilling in the joint planes dipping. This may cause the drilling bits to bind while they are operating in the joints, thus avoiding this overlap was essential. The crew members working the following shift at the drilling operation were given precise instructions on how to maintain the drilling precision for the succeeding blasts. Recorded blasts data presented in Table 1 (Figs. 5 and 6)

3 Results and Discussions

Phase I:

Table 1. Blast data

S.NO	Spacing Burden Ratio (Se/Be), m	Stemming Length, m (Times of B)	Maximum Charge/dela	Total Explosive, kg	Firing pattern	Distance Measurement,m	Joint Angle	Horizontal Joint spanning height	Joint Number Sets	MFS.m	PPV.mm/s
1	1.2	4.5	350	11,700	**3**	200	80	1.5	**1**	0.56	1.56
2	1.2	4.5	375	11,700	**3**	300	87	3.5	**1**	0.46	1.72
3	1.2	4.5	356	8,655	**3**	500	56	3	**1**	0.55	1.32
4	1.2	4.5	345	11,700	**3**	500	26	4	**1**	0.48	0.96
5	1.2	4.5	370	10,460	**2**	200	87	4	**1**	0.66	3.1
6	1.2	4.5	365	9,940	**2**	200	65	4.2	**2**	0.91	2.4
7	1.2	4.5	347	11,700	**2**	300	62	3	**2**	0.85	2.89
8	1.2	4.5	345	11,650	**2**	500	35	3.6	**2**	0.79	2.65
9	1.2	4.5	376	10,560	**1**	300	48	1	**2**	1.7	3
10	1.2	4.5	359	9,720	**1**	200	56	1.3	**2**	1.54	4.56
11	1.2	4.5	340	11,650	**1**	200	61	3	**3**	1.45	4.8
12	1.2	4.5	345	11,350	**1**	300	48	2.9	**3**	1.32	3.78
13	**1.2**	4.5	370	105460	**3**	300	87	1.4	2	0.42	1.87
14	**1.2**	4.5	367	11,600	**3**	500	29	2.7	1	0.52	2

(*continued*)

Table 1. (*continued*)

S.NO	Spacing Burden Ratio (Se/Be), m	Stemming Length, m (Times of B)	Maximum Charge/dela	Total Explosive, kg	Firing pattern	Distance Measurement,m	Joint Angle	Horizontal Joint spanning height	Joint Number Sets	MFS.m	PPV.mm/s
15	**1.2**	4.5	348	10,450	**3**	500	89	2.5	1	0.47	1.7
16	**1.2**	4.5	378	11,600	**3**	200	80	3.4	2	0.56	3
17	**1.25**	4.5	368	10,700	**3**	300	79	5.8	2	0.51	2.7
18	**1.25**	4.5	360	9,700	**3**	200	86	4.6	2	0.58	2.22
19	**1.25**	4.5	364	9,950	**3**	200	56	5.32	2	0.78	3.52
20	**1.25**	4.5	350	11,500	**3**	300	58	2	2	0.664	2.9
21	**1.3**	4.5	358	10,480	**3**	500	79	3.1	2	0.41	1.23
22	**1.3**	4.5	380	9,800	**3**	300	86	2	1	0.37	1.46
23	**1.3**	4.5	360	9,910	**3**	200	80	4.72	2	0.44	2.67
24	**1.3**	4.5	340	11,210	**3**	300	89	3.8	2	0.49	2.1
25	1.3	4.5	350	9,890	**3**	500	79	2	2	0.55	1.42
26	1.3	4.5	350	11,800	**3**	500	21	2.5	2	0.39	1.12
27	1.3	4.5	345	10,920	**3**	200	25	2.9	2	0.45	2.31
28	1.3	4.5	310	7,020	**3**	300	79	5.7	1	0.45	1.67
29	1.3	4.5	305	8,775	**3**	500	85	4.8	1	0.38	1.7
30	1.3	4.5	315	9,750	**3**	500	57	2	1	0.63	1.79
31	1.3	4.5	270	11,780	**3**	300	79	3.7	2	0.71	1.8
32	1.3	4.5	285	7,584	**3**	200	54	2	3	0.8	2.12

(*continued*)

Table 1. (*continued*)

S.NO	Spacing Burden Ratio (Se/Be), m	Stemming Length, m (Times of B)	Maximum Charge/dela	Total Explosive, kg	Firing pattern	Distance Measurement,m	Joint Angle	Horizontal Joint spanning height	Joint Number Sets	MFS.m	PPV.mm/s
33	1.3	4.5	290	7,810	**3**	300	79	2.1	1	0.48	2.8
34	1.3	4.5	335	**10,620**	**3**	500	86	2	2	0.45	1.21
35	1.3	4.5	300	**7,320**	**3**	500	81	2	1	0.56	1.04
36	1.3	4.5	2	**8,515**	**3**	500	80	2.4	1	0.56	1.31
37	1.3	4.5	315	**9,045**	**3**	200	65	2	3	0.9	3.21
38	1.3	4.5	325	**9,756**	**3**	200	57	2.6	3	1.2	4.21
39	1.3	4.5	330	**8,455**	**3**	300	45	1.4	3	0.89	3.21
40	1.3	4.5	245	**7,280**	**3**	200	48	5.21	3	0.94	4.21
41	1.3	4.5	250	**7,020**	**3**	300	65	6	3	0.711	3.37
42	1.3	4.5	255	**5.67**	**3**	200	69	5.7	3	0.743	4.21
43	1.3	4.5	315	**9,045**	**3**	200	78	5.32	3	0.71	3.02
44	1.3	4.5	325	**9,756**	**3**	300	84	1	2	0.52	3.18
45	1.3	4.5	330	**8,455**	**3**	500	70	3.2	1	0.47	2.14
46	1.3	4.5	245	**7,280**	**3**	500	69	3.9	2	0.621	1.26
47	1.3	4.5	200	**5,660**	**3**	500	65	4.72	2	0.55	0.95
48	1.3	4.5	205	**5,655**	**3**	300	66	3.8	1	0.41	1.02
49	**1.3**	4.5	195	5,645	**3**	500	57	2.1	1	0.76	0.92

(*continued*)

Table 1. (*continued*)

S.NO	Spacing Burden Ratio (Se/Be), m	Stemming Length, m (Times of B)	Maximum Charge/dela	Total Explosive, kg	Firing pattern	Distance Measurement,m	Joint Angle	Horizontal Joint spanning height	Joint Number Sets	MFS.m	PPV.mm/s
50	**1.3**	4.5	252	6,156	**3**	200	68	4.65	2	0.96	3.45
51	**1.3**	4.5	234	5,455	**3**	300	51	2	3	0.8	3.21
52	**1.3**	4.5	200	5,280	**3**	300	47	4	3	1.21	3.96
53	**1.3**	4.5	186	6,660	**3**	300	68	2.3	3	0.95	2.3
54	**1.3**	4.5	231	6,655	**3**	500	53	2	3	1.1	1.34
55	**1.3**	4.5	200	5,045	**3**	200	76	2	3	0.79	3.61
56	**1.3**	4.5	200	5,656	**3**	300	70	2.7	3	0.63	2.4
57	**1.2**	4.5	245	5,580	**1**	300	71	2.1	2	0.84	2.3
58	**1.2**	4.5	189	5,260	**1**	500	78	2.04	2	0.73	1.34
59	**1.2**	4.5	190	5,555	**1**	200	80	5	2	0.59	3.61
60	**1.2**	4.5	189	6,480	**1**	300	58	3	3	0.94	2.2
61	1.2	4.5	231	**10,140**	**3**	200	60	3	2	0.7	3.1
62	1.2	4.5	200	**11,707**	**3**	200	49	5.4	2	0.65	2.56
63	1.2	4.5	200	**9,350**	**3**	200	80	2.6	2	0.49	2.98
64	1.2	4.5	245	**7,110**	**3**	300	37	3.7	3	0.83	1.6
65	1.2	4.5	189	**7,310**	**3**	300	49	4	3	0.9	1.62
66	1.2	4.5	231	**8,100**	**3**	200	84	4.3	3	0.58	3.64

(*continued*)

Table 1. (*continued*)

S.NO	Spacing Burden Ratio (Se/Be), m	Stemming Length, m (Times of B)	Maximum Charge/dela	Total Explosive, kg	Firing pattern	Distance Measurement,m	Joint Angle	Horizontal Joint spanning height	Joint Number Sets	MFS.m	PPV.mm/s
67	1.2	4.5	275	**6,770**	**3**	500	70	4	2	0.64	1.69
68	1.2	4.5	204	5,156	**3**	500	79	1.2	3	0.6	1.46
69	1.2	4.5	179	5,580	**1**	500	48	5	3	1.21	1.96
70	1.2	4.5	189	5,260	**1**	300	60	1.32	3	0.99	2.13
71	1.2	4.5	190	5,555	**1**	200	53	5.34	2	1.89	3.19
72	1.2	4.5	158	**6,900**	**1**	500	58	3	3	1.67	1.35
73	1.3	4.5	310	**8,800**	**3**	300	75	3.12	2	0.95	1.78
74	1.3	4.5	315	**9,830**	**3**	500	63	2	3	0.81	1.12
75	1.3	4.5	320	**8,521**	**3**	300	58	2.4	2	0.63	2.1
76	1.3	4.5	290	**7,255**	**3**	300	60	2.1	2	0.57	2.1
77	1.3	4.5	255	**7,200**	**3**	500	69	3	2	0.44	1.57
78	1.3	4.5	215	**5,940**	**3**	200	88	3	2	0.52	2.11
79	1.3	4.5	312	**8,521**	**3**	200	86	2.5	3	0.78	2.31
80	1.3	4.5	250	**7,255**	**3**	500	69	3	2	0.71	1.12
81	1.3	4.5	312	**7,200**	**1**	500	74	1.1	2	0.91	1.56
82	1.3	4.5	185	**5,940**	**1**	500	77	4.3	2	0.26	1.64
83	1.3	4.5	195	**5,700**	**1**	200	16	4.1	2	0.37	1.84
84	1.3	4.5	220	**5,660**	**1**	200	18	4	2	0.29	2.11

(*continued*)

Table 1. (*continued*)

S.NO	Spacing Burden Ratio (Se/Be), m	Stemming Length, m (Times of B)	Maximum Charge/dela	Total Explosive, kg	Firing pattern	Distance Measurement,m	Joint Angle	Horizontal Joint spanning height	Joint Number Sets	MFS.m	PPV.mm/s
85	1.2	4.5	380	9,890	**3**	500	80	1.5	**1**	0.6	0.95
86	1.2	4.5	370	9,950	**3**	500	87	3.5	**1**	0.47	1.21
87	1.2	4.5	390	8,655	**3**	500	56	3	**1**	0.42	1.86
88	1.2	4.5	359	9,730	**3**	300	26	4	**1**	0.42	1.42
89	1.2	4.5	378	9,460	**2**	200	87	4	**1**	0.99	2.67
90	1.2	4.5	330	9,890	**2**	200	65	4.2	**2**	0.94	3.1

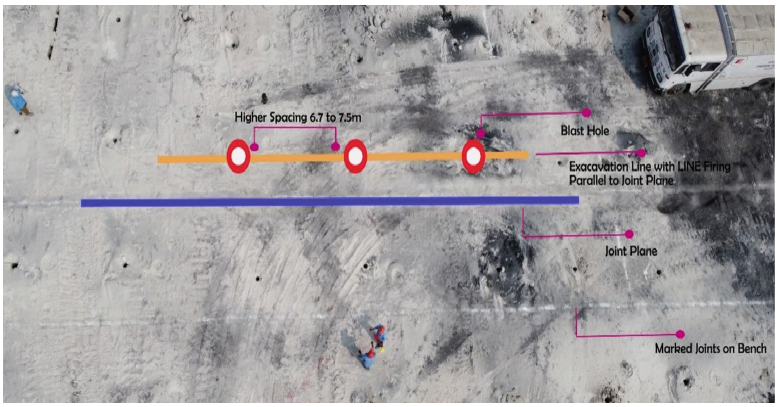

Fig. 5 Line firing for parallel joints with higher spacing at opencast coal mines at ramagundam III, SCCL.

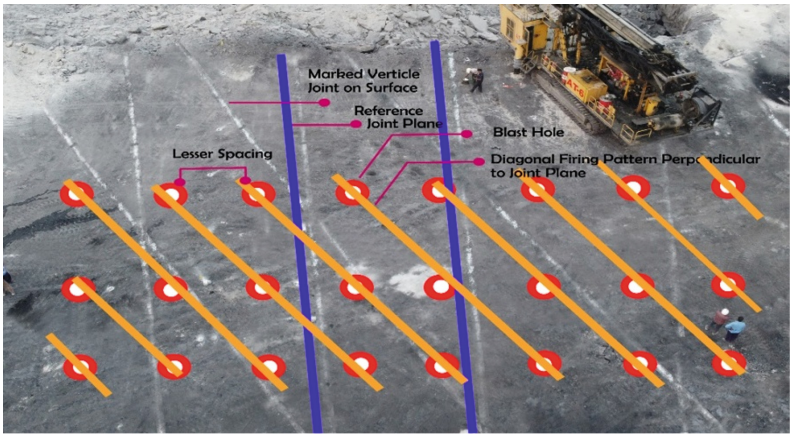

Fig. 6 Diagonal firing for vertical joints with lesser spacing at opencast coal mines at ramagundam III, SCCL.

Effect of Firing Pattern on Mean Fragmentation Size and Peak Particle Velocity

In Phase I, three firing patterns were performed to determine the influence of firing pattern on simultaneous blast results such as mean fragmentation size and peak particle velocity. Rectangular drilling with a line firing pattern was chosen to fire blasts parallel when joints are parallel to the free face to permit appropriate in-flight collision, as indicated in picture 8.1. Similarly, Diagonal and V firing patterns were chosen to ease shooting perpendicular to the free face to achieve improved breakage and rock displacement, as indicated in picture 8.2. A total of 90 blasts were conducted to explore the influence of firing patterns on blasting outcomes.

Each firing pattern was selected based on the direction of joint presence on the bench surface and face. As shown in Figs. 7 and 8, for each blast in Phase I, joints have been highlighted in accordance with the joints found in AI-based software. In all three

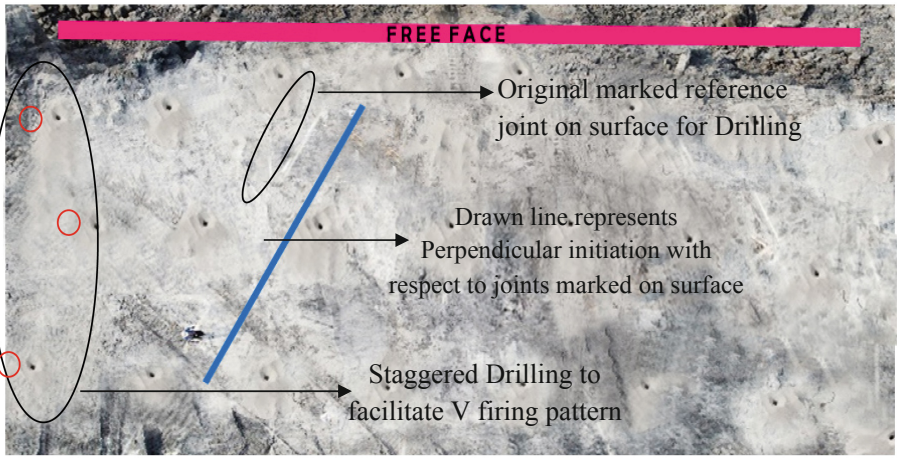

Fig. 7 V Firing with respect to joints perpendicular to free face

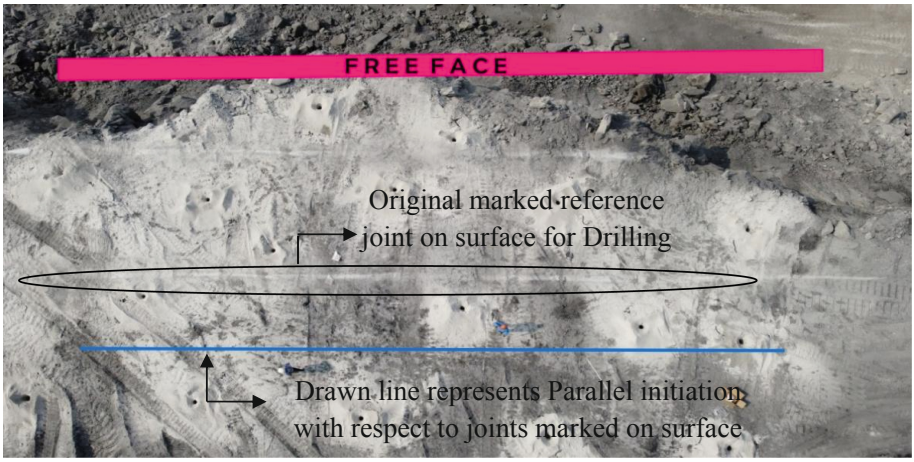

Fig. 8 Line Firing with respect to joints parallel to free face

investigation mines, the number of surface joints varied from bench to bench (Figs. 9 and 10).

From Fig. 11 (a&b), it is observed that in all three firing patterns, V produced good fragmentation sizes hovering between 0.41 to 0.56m, perpendicular firing initiation with the V pattern reduced hole burdens and increased spacing at the time of hole initiation and in-flight collision of broken rock during its movement, lowest MFS 0.41mm can be seen in Fig. 10(b). In other circumstances, the existence of several joint clusters inclined away from the vertical face causes gravity force to induce rock displacement when gas energy enters through joints. In the case of PPV, safe PPV was produced between 0.95 to 3.1mm/s in different monitoring distances with a V firing pattern due to the cancellation of the wave patterns generated by simultaneous holes on both the arms of the V as

Fig. 9 Photograph of fragmentation with Line firing pattern & V firing pattern

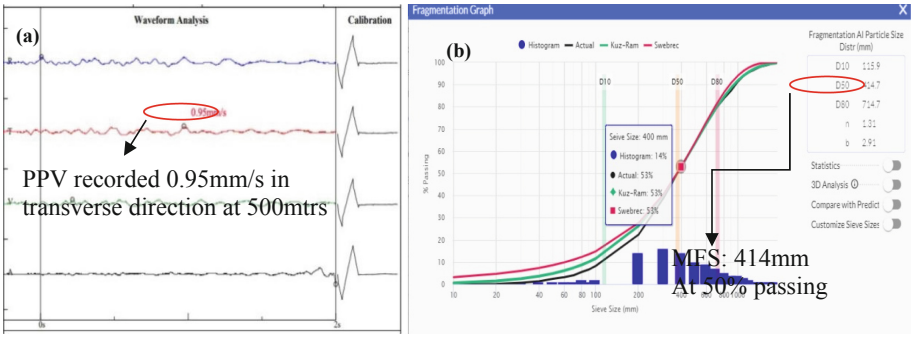

Fig. 10. PPV waveform and Fragmentation Curve

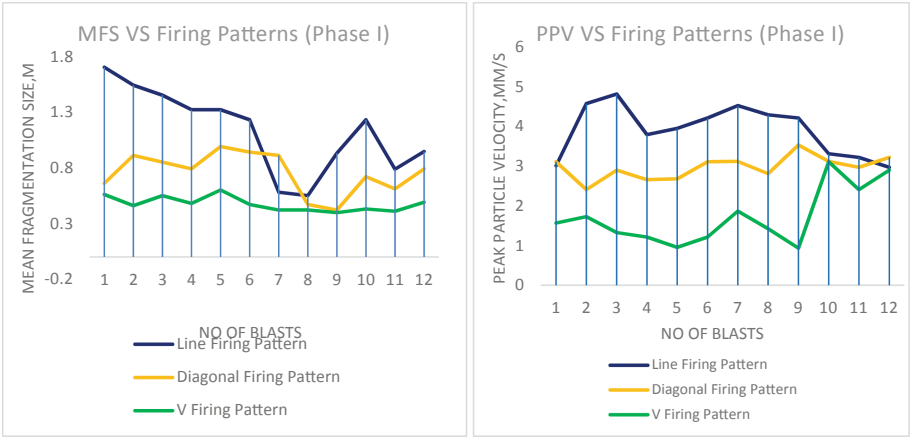

Fig. 11 Relation between MFS - Firing Pattern & PPV- Firing Pattern

compared to diagonal or line firing patterns, except few blasts PPV little higher due to presence of only one joint set causing no attenuation rather rock absorption. Lowest PPV recorded was 0.95mm/s as shown in Fig. 10(a).

Phase II:

Effect of Spacing Burden Ratio on Mean Fragmentation Size and Peak Particle Velocity:

In Phase II, three S/B ratios were used to provide for a larger spacing burden ratio where joints are parallel to the free face as shown in Fig. 12, and a lower spacing burden ratio in which joints are perpendicular to the free face as shown in Fig. 13. Three S/B ratios 1.2, 1.25 & 1.3 were investigated to see how the spacing burden ratio affected simultaneous blast results like mean fragmentation size and peak particle velocity (Fig. 14).

From Fig. 16, it is observed that dominant joints parallel the face, a larger spacing burden ratio of 1.3 resulted in excellent fragmentation of 0.4 m shown in Fig. 15b by preventing early joint integration and superficial crater fracturing and the maximum MFS obtained was 720 mm shown in figure 9.8b. Similarly, PPV is also produced at 1.23 shown in figure 15a due to impedance mismatch in transmission wave caused reflection instead of following propagation path due to the number of joints presence in bench, the increment in PPV in the same trend is however due to change in various monitoring distances.

In the case of vertical joints that are perpendicular to the excavation face, a lower spacing burden ratio of 1.2 resulted in good mean fragmentation sizes ranging from 0.4 to 0.6, except for two blast results that may be due to seismic wave reflection and refraction caused by crossing with many inclined joints and the maximum MFS produced was 800 mm which shown in figure 9.8a.

A lower S/B ratio aided early rock breakup by retaining seismic energy before it escaped from the peripheral joints. Analogously, PPV is slightly higher than 1.3 S/B ratio adoptions, which could be attributed to the confinement of shock - gas energies with a 1.2 S/B ratio to break and displace rock rather than attenuation and wastage of explosive energy facilitated as a scaffold to pass seismic wave and accelerated marginally greater PPV.

Phase III:

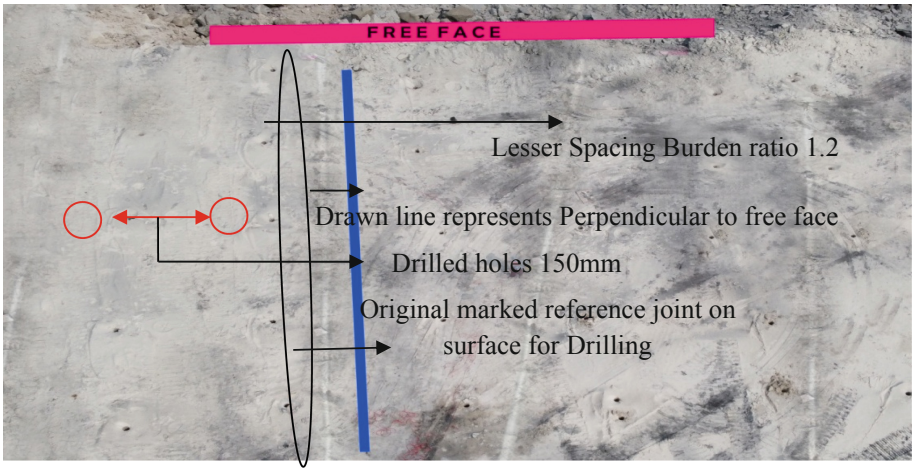

Fig. 12 Less spacing Burden when joints parallel to free face

Fig. 13. Higher spacing Burden when joints perpendicular to free face

Fig. 14 Photograph of fragmentation with S/B ratio 1.2 & S/B ratio 1.3

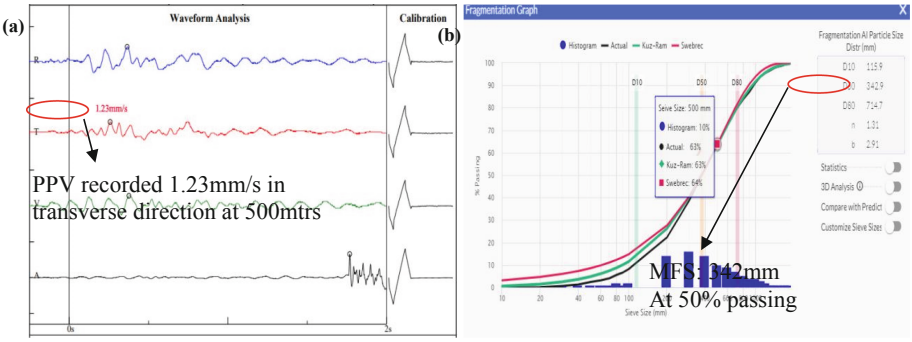

Fig. 15 PPV waveform and Fragmentation Curve

Effect of Spacing burden ratio and Firing Pattern on Mean Fragmentation Size and Peak Particle Velocity:

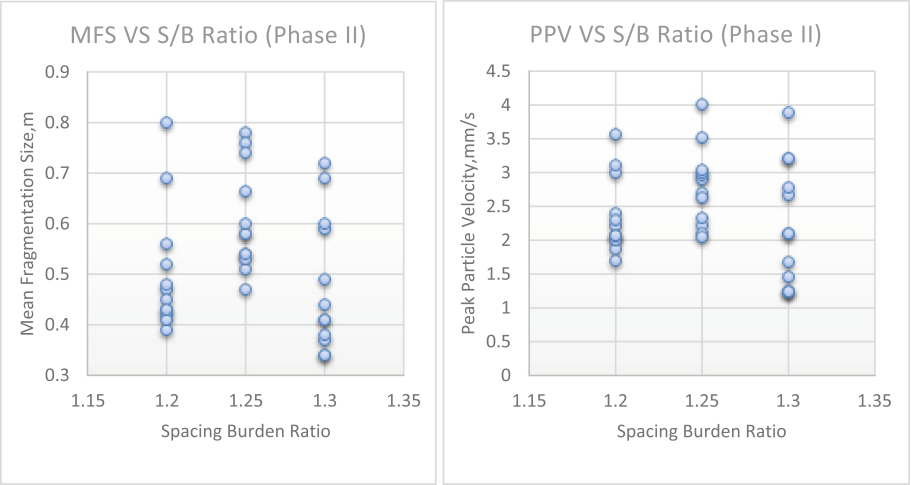

Fig. 16 Relation between MFS - Spacing Burden Ratio & PPV - Spacing Burden Ratio

In Phase V, the combination of spacing burden ratio and firing pattern was examined simultaneously since it is vital to design blast in conjunction with the rock's geology and structural parameters. The spacing burden ratios of 1.2 and 1.35, as well as the firing patterns line and V, were repeated since they yielded superior blasting outcomes in prior phases. Stemming length of 0.9 times burden (4.5m) and decking length of 4m were pulled from earlier phases and maintained constant since they produced better outcomes. Preferences for S/B ratio and firing pattern were comparable to Phase I and II concerning joint presence on the bench surface and free face.

The link between MFS and the combined impact of S/B and the firing pattern is depicted in Fig. 19 (a&b). The position of the joints was indicated on the bench surfaces, and the placement of holes was done with the S/B ratio in mind, and holes were not placed too near to joints. According to the findings, MFS decreases with decreasing S/B ratio of 1.2, most likely due to successful utilization of explosive energy due to collision of the wave pattern established in the contiguous holes, which aids in better rock fragmentation. Line firing with 1.2 S/B provided MFS 0.598 m as shown in Fig. 18b, which might be attributed to perpendicular firing concerning vertical joint (approximately 90^0), which aided in-flight collision of rock shattered during its movement and resulted in a lower S/B ratio. As in Phase II presented, 1.2 S/B helped early rock breakage by holding seismic energy before it flowed from the peripheral joints. Maximum MFS observed with a 1.2 S/B ratio is 840mm and a 1.35 S/B ratio is 1.28 m as shown in Fig. 18 (a&b). Similarly, the PPV trend was equal with both 1.2 and 1.35 ratios and Line and V Firing patterns, implying that the lower S/B ratio accelerated less attenuation and PPV produced approximately 0.93 mm/s as shown in Fig. 17.

Phase IV:

Effect of Joint Angle on Mean Fragmentation Size and Peak Particle Velocity:

The major joint pattern makes an angle ranging from 0 degrees when coinciding with the blast face and 90 degrees when perpendicular to the bench face.

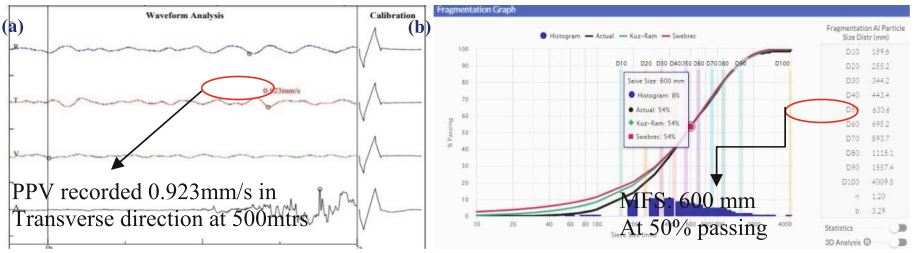

Fig. 17 PPV waveform and Fragmentation Curve

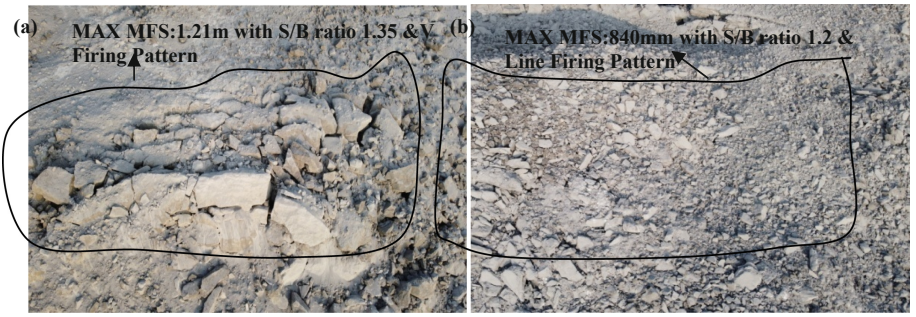

Fig. 18 Photograph of fragmentation with S/B ratio 1.35 - V firing pattern & S/B ratio 1.2 - Line Firing Pattern

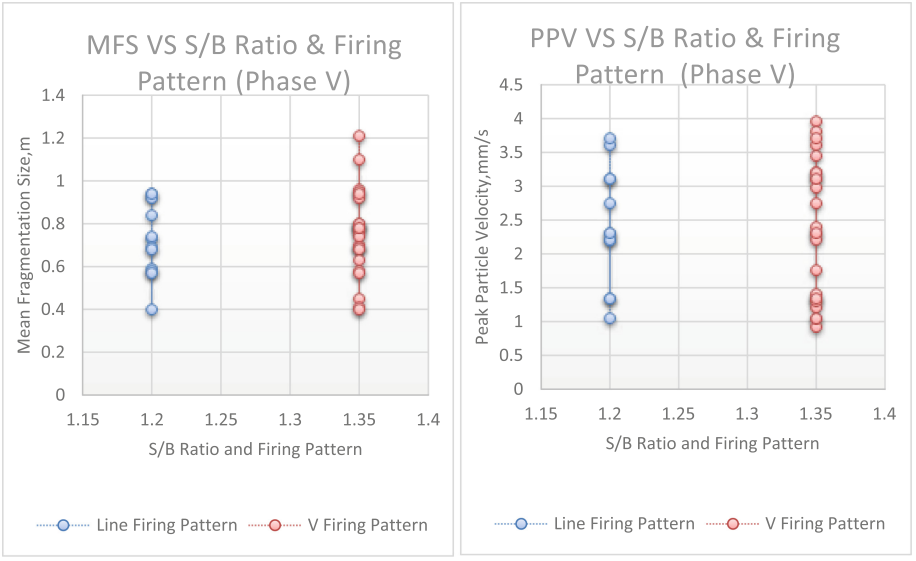

Fig. 19. Relation between MFS - Spacing Burden Ratio - Firing Pattern & PPV- Spacing Burden Ratio - Firing Pattern

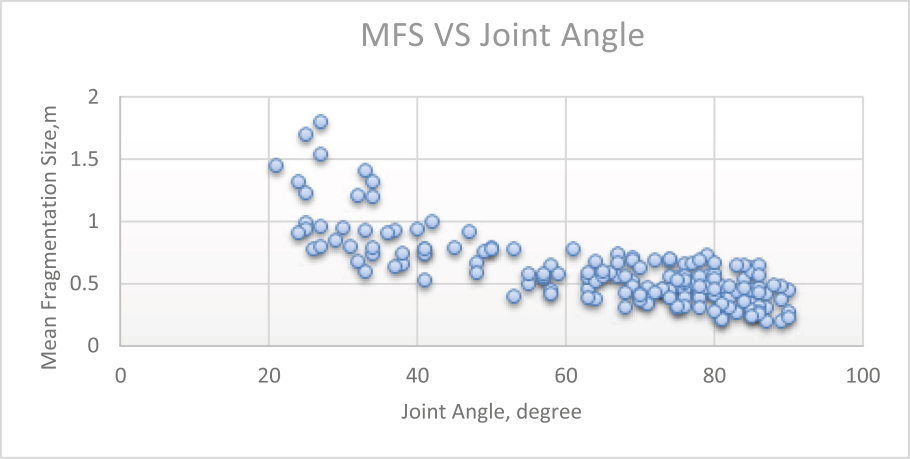

Fig. 20 Relation between MFS & Joint Angle

When studied the blast trials showed less MFS when the Joints are oriented in between 70–90° as shown in Fig. 20. The blast energy is better utilized when there is complete collision of the propagating and reflecting shock waves and so maximum result and less MFS occurs.

The angle between the line of shot holes and the joints influences the effectiveness of the blast which is indicated by the relative measure of the PPV. During the blast trials, it was observed that when the angle progressively increased there is a corresponding decrease in the PPV indicating the most effective blasts at angles 90 shown in Fig. 21. This may be due to the reason that the incident and the reflective blast wave meat squarely when the angle between them is 90 degrees. This corroborates observations of various previous authors. In all trials of Phase VII in a combination of change decking length and V firing along with the considerations of joint angle and rock compressive strength showed significant results of MFS below 0.3 m with and PPV produced lower than 0.7mm/s with decking length 4m and V firing pattern.

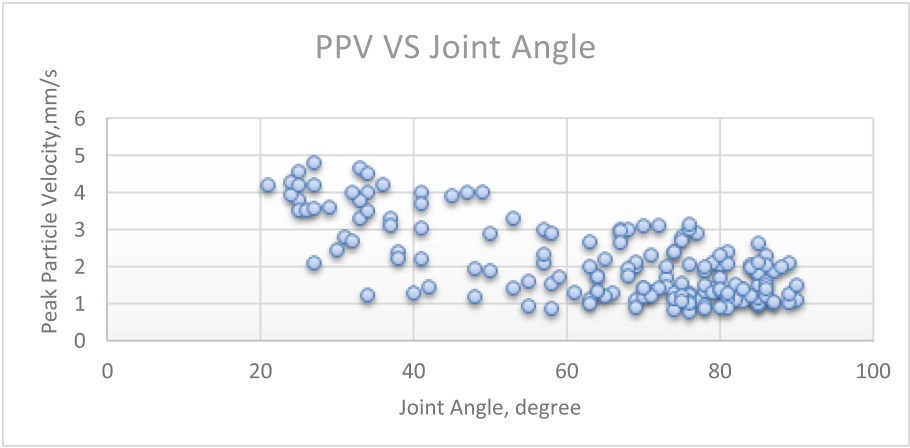

Fig. 21 Relation between MFS & Joint Angle

4 Conclusion

- From the study, it was found that mean fragment sizes (MFS) and peak particle velocity (PPV) are affected by geotechnical characteristics such as joint angle, joint number, joint spanning height, and rock compressive strength.
- An Unmanned Aerial Vehicle (UAV) is a good tool to capture images. These images were used to identify rocks, plan blasts, determine the size of benches, and gauge the volume of muck.
- In the present study state-of-art AI-based software, was well assisted in evaluating rock mass characteristics such as joint dip-strike directions and joint dip angle which greatly helped in creating many blasts.
- AI-based design software was used to help in blast design and offer early warnings for iterations.
- It was found that the V initiation pattern produced better fragmentation ranging between 0.49 to 0.56, as opposed to a line or diagonal.
- In terms of PPV, it was observed that V firing pattern yield safe values between 0.49 to 2.89 mm/s at various distances.
- In the case of the S/B ratio, 1.3 created fragmentations between 0.34 to 0.72 m, which enabled, shovel loading easier and fast.
- It was found that 1.3 S/B ratios produced PPV between 1.23 to 3.89 mm/s.
- It was revealed that the combination of S/B ratio 1.2 and V firing pattern produced good mean fragmentation size values ranging from of 0.59 to 0.84.
- In the case of PPV, it was found the combination of S/B ratio 1.2 and the V firing pattern brought PPV values between 1.34 mm/sec to 3.61 mm/sec.

References

1. Rai, P. (2002). Evaluation of effect of some blast design parameters on fragmentation inopencastmine. Ph.D. thesis, Banaras Hindu University, Varanasi.

2. McKenzie, C.K. (1999). A review of the influence of gas pressure on block stability duringrockblasting, Procs. Explo-99, Kalgoorlie, WA, pp: 173–179.
3. Stagg, M.S., Otterness, R. & Siskind, D.F. (1992). Effects of blasting practices on fragmentation, Rock Mechanics, Titherson Ed., Balkema, Rotterdam, pp: 313–322. 33rd U.S. Symposium on Rock Mechanics (USRMS), Santa Fe, New Mexico, June 1992. Paper Number: ARMA-92–0313 Published: June 03.
4. Adamson, W.R., Scherpenisse, C.R. & Diaz, J.C. (1999).The use of blast monitoring modeling technology for the optimization of development blasting, Proc.Explo-99, Kalgoolie, WA, pp: 35–41.
5. Kanchibotla, S.S.,Valery,W. & Morrell, S. (1999). Modelling fines in blast fragmentation and its impact on crushing and grinding, Procs.Explo-99, Kalgoorlie, Western Australia, pp: 137–144.
6. Bhandari, S. (1997). Engineering rock blasting operations, A.A. Balkema, Rotterdam, The Netherlands.
7. Sri N. Chandrahas, B.S. Choudhary, N.S.R. Krishna Prasad, V. Musunuri, K.K. Rao, An Investigation into the Effect of Rockmass Properties on Mean Fragmentation. Arch. Min. Sci. 2021, 66, 561–578.
8. Chiappetta, R.F., Borg, D.G. & Sterner, V.A. (1987). Explosives and rock blasting. Atlas Powder Company, Dallas, pp:233.
9. Hagan, T.N. (1983). The influence of controllable blast parameters on fragmentation and mining costs, In: Proceedings of the 1st International Symposium on Rock Fragmentation by Blatssting1, 31–32.
10. Persson, P.A., Lundborg, N. & Johansson, C.H. (1970). The basic mechanism of rock blasting. Proc. 2nd Cong. Int. Soc. Rock Mechanics, Belgrade, Vol-3, pp: 19–33.
11. Hino, K. (1956). Fragmentation of rock through blasting and shock wave theory of blasting. Quart. Colorado School of Mines 51 (1956) (1), pp: 189–209 The 1st U.S. Symposium on Rock Mechanics (USRMS), Golden, Colorado, April 1956. ARMA-56–0191.
12. Duvall, W. I. & Atchison, T. C. (1957). Rockbreakagebyexplosives,USBMRI5356.
13. Fourney, W.L. (1993). Mechanisms of rock fragmentation in by blasting. Hudson J.A, editor. Compressive rock engineering, principles, practice and projects. Oxford: PergamonPress.
14. Ash, R.L. (1973). The influence of geological discontinuities on rock blasting, Ph.D. thesis, Univ. of Missouri, USA.
15. Konya, C.J. (1990). Designing blasts with uncertainity and tolerance. Proc. 16th confr. One xplosives and blasting techniques, Society of Explosive Engineers, Orlando, Florida.
16. Clark, G.B. (1987). Principles of Rock Fragmentation, John Wiley & Sons Inc., London.
17. Fengpeng Zhang (2015). Optimization of blasting parameters for an underground mine through prediction of blasting vibration. Journal of Vibration and Control. DOI: https://doi.org/10.1177/1077546319829938
18. Rinehart, J.S. (1958). Fracturing under impulsive loading, 3rd Ann. Symp. Min. Res., Univ. MoSchool Min, Metall. Tec. Series No. 95, p: 46.
19. Davis, G.H., S.J. Reynolds. & C, Kluth. (2012). Structural Geology of Rocks and Regions (3rd ed.): John Wiley and Sons, Inc., New york, New York. 864 pp. ISBN 978–0471152316
20. Goudie, A.S. (2004). Encyclopedia of Geomorphology volume 2 J–Z. Routledge New York, New York. 578 pp. ISBN 9780415327381
21. Goodman, R.E., Taylor, L. & Brekke, T.L. (1968). A model for the mechanics of jointed rock. J Soil Mech Found Div, ASCE 94(SM3):637–659.
22. Burkle, W.C. (1979). Geology and its effect on blasting. In: Proceedings of the 5th conference on explosives and blasting techniques, SEE, pp 105–120.
23. Cundall, P.A. (1990). Numerical modelling of jointed and faulted rock. In: Rossmanith HP (ed) Mechanics of jointed and faulted rock. A.A. Balkema, Rotterdam.

24. Worsey, P.N. & Qu. S (1987). Effect of joint separation and filling on pre-split blasting. The 3rd Mini Symposium on Explosives and Blasting Research. pp. 26–40.
25. Whittaker, B.S., Singh, R.N. & Sun, G. (1992). Fracture Mechanics Applied to Rock Fragmentation due to blasting. Rock Fracture Mechanics—Principles, Design and Applications, Elsevier Science Ltd. 71 (13), 443–479.
26. 27. J.C. Li., Li H.B. & Zhao, J. (2015). An improved equivalent viscous-elastic medium method for wave propagation across layered rock masses. Int. J. Rock Mech. Min. Sci. DOI: http://dx.doi.org/https://doi.org/10.1016/j.ijrmms.2014.10.008.
27. Vinh, P.C., Tuan, T.T., Tung, D.X. & Kieu, N.T. (2017). Reflection and transmission of SH waves at a very rough interface and its band gaps. J. Sound Vib. 411–422 DOI: https://doi.org/10.1016/j.jsv.2017.08.046.
28. Maerz, N.H., Franklin, J.A., Rothenburg, L. & Coursen, D.L. (1987). Measurement of rock fragmentation by digital photo analysis, 5th Int. Congr. Int. Soc. Rock Mech, pp: 687–692.
29. Bhandari, S. (1975). Burden and Spacing Relationship in the Design of Blasting pattern. 16th Symp. Rock Mechanics, University of Minnesota, pp 333–343
30. Hagan, T.N. (1983) The influence of controllable blast parameters on fragmentation and mining costs, In: Proceedings of the 1st International Symposium on Rock Fragmentation by Blatssting1, 31–32.
31. Sandeep Prasad, B.S. Choudhary, A.K. Mishra. Effect of Blast Design Parameters on Blast Induced Rock Fragmentation Size – A Case Study. Int. Conf. on Deep Excavation, Energy Resources and Production DEEP16 24–26 January 2017, IIT Kharagpur, India
32. Langefors, U & Kihlstrom, B. (1978). The modern technique of rock blasting, Editor, John Wiley and Sons Inc., NewYork, pp.438.
33. Malcolm Scoble., Yves Lizotte., Mario Paventi & ChantaleDoucet. (1960). Measurement of Blast Fragmentation, Franklin & Katsabanis (eds), Balkema, Rottedam. ISBN:9054108452.
34. Smith, N.S. (1976). An investigation of the effects of blast hole confinement on generation of ground vibration in bench blasting, Final report for blasting research, SMI grant section, 301.
35. Rai, P. & Baghel, S.S. (2004). Investigation of firing patterns on fragmentation in an Indian open cast limestone mine. Quarry Management Journal, February, pp 21–30.
36. 37. Belland, J.M. (1968). Structure as a Control in Rock Fragmentation Coal Lake Iron Ore Deposited. The Canadian Mining and Metallurgical Bulletin. 59 (647), 323–328.
37. 38. Talhi, K. & Bensaker, B. (2003). Design of a model blasting system to measure peak p-wave stress, Soil Dyn. Earthq. Eng. 23 (6), 513–519, DOI: http://dx.doi.org/https://doi.org/10.1016/S0267-7261(03)00018-6.
38. Sri Chandrahas, N., Bhanwar Singh Choudhary., Vishnu Teja, M., Venkataramayya, M.S. & Krishna Prasad, N.S.R. (2022). XG Boost Algorithm to Simultaneous Prediction of Rock Fragmentation and Induced Ground Vibration Using Unique Blast Data. *Appl. Sci.*, *12*(10), 5269; DOI: https://doi.org/10.3390/app12105269.
39. 40. Turner, D., Lucieer, A., Watson, C. (2012). An automated technique for generating geo-rectified mosaics from ultra-high resolution Unmanned Aerial Vehicle (UAV) imagery, based on Structure from Motion (SfM) point clouds. Remote Sens. 4, 1392–1410, http://dx.doi.org/https://doi.org/10.3390/rs4051392.
40. 41. Thomas Bamford, Kamran Esmaeili & Angela, P., Schoellig (2017): A real-time analysis of post-blast rock fragmentation using UAV technology, International Journal of Mining, Reclamation and Environment, DOI: https://doi.org/10.1080/17480930.2017.133917
41. Kottenstette, J. (2005). Measurement of geologic features using close range terrestrial photogrammetry. In: Proceedings of the 40th US Symposium on Rock Mechanics (USRMS) Alaska Rocks.

42. 43. Cruden, A., Vollgger, S., Dering, G., & Micklethwaite, S (2016). High Spatial Resolution Mapping of Dykes Using Unmanned Aerial Vehicle (UAV) Photogrammetry: New Insights On Emplacement Processes, Acta Geol. Sin.-Engl., 90, 52–53, https://doi.org/https://doi.org/10.1111/1755-6724.12883.
43. 44. Yathunanthan Vasuki, n., Eun-Jung Holden, Peter Kovesi, Steven Micklethwaite (2014). Semi-automatic mapping of geological Structures using UAV-based photogrammetric data: An image analysis approach. Computers & Geosciences . DOI:https://doi.org/10.1016/j.cageo.2014.04.012
44. 45. Thiele, S.T., Grose, L., Samsu, A., Micklethwaite, S., Vollgger, S. A., & Cruden, A. R. (2017). Rapid, semi-automatic fracture and contact mapping for point clouds, images and geophysical data. Solid Earth, 8(6), 1241–1253. https://doi.org/https://doi.org/10.5194/se-8-1241-2017
45. 46. Yang, X-S (2009). Firefly algorithms for multimodal optimization. In: International symposium on stochastic algorithms. Springer, Berlin, pp 169–178
46. 47. M. Hajihassani, D. J. Armaghani, M. Monjezi, M. E. Tonnizam, A. Marto (2015). Blast-induced air and ground-vibration prediction: A particle swarm optimization-based artificial neural network approach. Environmental Earth Sciences, 74(4), 2799–2817.